Wake Patterns around Front Tire and Wheel on Vehicle Dynamics Clarified by On-Board PIV Application

N. Kuratani[1*], T. Kawamura[2], K. Ambo[2]
1: Innovation Research Excellence, Honda R&D Co., Ltd, Japan
2: Automobile Operations Monozukuri Center, Honda Motor Co., Ltd, Japan
* Correspondent author: Naoshi_Kuratani@jp.honda

Keywords: Wake Pattern, Rotating tire and wheel rotation, Onboard PIV, POD

ABSTRACT

Temporal and spatial wake patterns and behaviors around rotating tires and wheels are some of the most critical flow phenomena on aerodynamic performance and vehicle dynamics. In particular, aerodynamic drag is one of the most important factors on greenhouse effect gas and fuel efficiencies, in these days remarkably focused on the shift from conventional fossil fuel power plants to electric ones to prevent the global warming. From the point of view of aerodynamics, OEMs' wind tunnel facilities with moving ground and high fidelity CFD tools are employed to optimize the exterior body shape and aerodynamic device in order to reduce the aerodynamic drag. Recently, high fidelity CFD tools which include tire rotations are easily employed by users, not only specialists, to analyze the flow around the vehicle and to optimize the exterior design at the development phase. However, more accurate and detailed understanding of complicated flow phenomena around vehicle during motion are required to predict these flow phenomena accurately by CFD tools at early development phase. Moreover, the more detailed experimental investigation is essential for the aerodynamicists, not only to develop the prediction tool but also to understand the flow phenomena around vehicle in its essence. Therefore, in this study, the on-board 2D-3C PIV measurement system in wind tunnel facility has been developed to investigate the wake patterns around rotating front tire and wheel. As result, the critical wake patterns have been clarified by POD analysis of the mentioned on-board 2D-3C PIV measurement data. These front wheelhouse wake patterns were classified in terms of the wake generation locations that produced the aerodynamic drag. These results indicate that there is the potential for an improvement in not only aerodynamic drag and but also vehicle dynamics by flow control to suppress the wake generations around front wheelhouse and the flow fluctuation around bodyside, moreover, this system can be applied to real world running condition in near future.

1. Introduction

Various needs of customers, new laws and regulations for the next generation of launching vehicles must be satisfied all over the world. These customers' needs are regional and time-dependent; moreover, the vehicles must be timely delivered to a market with competitiveness

with respect to other manufacturers by improving in terms of efficient research and development process while keeping development cost down. Recently, computer aided engineering is an essential and powerful tool for industrial product development. As well known, computational fluid dynamics, CFD, is one of powerful tools in the field of aerodynamics and aeroacoustics to promote the industrial research and development process (Ambo 2017, Ambo 2020). There is, in particular, still an unknown aerodynamic phenomenon in the real world due to wide and complicated design spaces. In these days, the wind tunnel facilities with moving ground are already actively used at research and development phase by automobile companies. These can simulate the real-world conditions as closely as possible, if not perfectly; single moving ground belt simulate the flow around under floor and rotating tire more precisely. Some aerodynamic devices underneath the vehicle floor are effective to reduce the aerodynamic drag and lift by controlling the body side wake and rear wake behind vehicles. Moreover, the tire rotation makes the complicated flow around not only tire, wheel, wheel-house area but also vehicle body.

The rotating wheels' effect on vehicle aerodynamics were studied or are still ongoing. The moving ground and rotating rear wheels affect much of the drag reduction due to the change in the interference of the wheel and wheel housing wakes with the vehicle base wake (Elofsson 2002). Several wheel rim geometries were examined in stationary and in rotating condition by CFD with MRF method, LDV and aerodynamic forces (Waschle 2007). The liability to flow separation at the wheel contact patches is reduced under rotating condition, which leads to smaller wheel squash vortices. As results, less air is pulled into the wheelhouse, which reduces the flow losses generated by the air leaving the wheel arch at the gap between the wheel arch and the upper part of the wheel. And the largest part of the changes in drag and lift due to rotating wheels must be attributed to interference between the underbody flow and the wakes of the rear wheels. Moreover, high fidelity CFD based on LES were developed and performed by validating the side wake patterns with different shapes of tire shoulder, and it clarifies that there is strong effect of side wake on vehicle aerodynamics (Takeuchi 2016). The flow topology in wheelhouse was analyzed and clarified by CFD with immersed boundary method (Hurlbrink 2019). In particular, streamwise component of the Lamb vector proved to be most appropriate for local drag analyses. These vortices could be identified which are sources of induced drag in the wheel-house area. There is one of remarkable application of PIV measurement to on road test (Haff 2017). This study was focused on the influence of a tunnel paneling and a simulated radiator shutter on the flow characteristics, especially mass flow rate, underneath vehicle via PIV.

In the conventional method, the velocity flow field around vehicle was captured by propagating a laser from the vehicle outside in wind tunnel, but the laser reflection on vehicle surface was not ignored. Furthermore, since this PIV measurement system due to complex and large one is limited to the inside of the wind tunnel. In this study, we tried to develop an onboard PIV measurement system considering an application in the real world driving to investigate the temporal and spatial flow phenomena around vehicle. The purpose of this study is to clarify the wake patterns, generation locations and temporal and spatial behaviors around rotating front tire and wheel by onboard time-series 2D-3C PIV measurement and POD analysis (Taira 2017). These experimental results can assist the aerodynamic optimization at early development phase for not only drag reduction but also improvement in vehicle dynamics and CFD tool to predict the complicated flow phenomena around vehicle under real world conditions.

2. Experimental Apparatus and Conditions

2.1. Wind Tunnel with Single Moving Ground Belt

The wind tunnel experiments were performed in the wind tunnel (Koremoto 2010, Koremoto 2011) owned by Honda R&D Co., Ltd. This wind tunnel has open jet type and a 6.7 x 3.6 [m^2] 3⁄4 nozzle, and this test section is 14.5 [m] length. The fan in this wind tunnel has maximum power of 3.6 [MW] and produces 1,400 [m^3/s] with 8 [m] diameter and 24 rotor vanes made with carbon fiber-reinforced plastic and 35 stator vanes with steel. The feature of this wind tunnel facility is a single moving belt system to simulate the running conditions. This single belt has 3.2 [m] width and 9 [m] length, that is distance between front and rear rollers, and 1 [mm] thickness of stainless-steel belt. And this single moving belt can be operated up to 300 [km/h]. And a boundary layer removal system has primary scoop for removing the developed boundary layers at the exit of nozzle and secondary suction and tangential blowing upstream of the single belt. Aerodynamic force measurement system has combined horizontal force and wheel force measurement systems. The former one can measure the drag and side force at the structural members of single moving belt system, the latter one can measure lift force by load cells installed under stainless steel belt with air bearing system, respectively. Test vehicle is always fixed by four hub bearings, but in this study, only one hub and rod are removed to investigate the two posts on single moving belt.

2.2. Test Vehicle and Configurations

The 10th Generation *CIVIC* (Honda Motors Co. Ltd.,) as compact sedan (*Length*=4,650 [mm], *Width*=1,800 [mm], *Height*=1,415 [mm]) was used for wind tunnel test in this study as shown in

Fig. 1. However, in this study only one hub bearing and rod at front side was removed not to disturb the flow around rotating tire and wheel as shown in Fig. 1 in detail. The coordinate system shows x-axis shows streamwise direction, y-axis lateral one and z-axis vertical one in Fig. 1. The Front Strake in front of front tire is used for drag reduction. And Grille Close indicates that the incoming flow into engine room for cooling system will be shut down, that causes to reduce the aerodynamic drag and to produce the negative front lift force due to this flow coming into the underfloor to increase the mass flow rate as shown in Fig. 2. These three configurations including baseline are compared to investigate the wake patterns around rotating front tire and wheel.

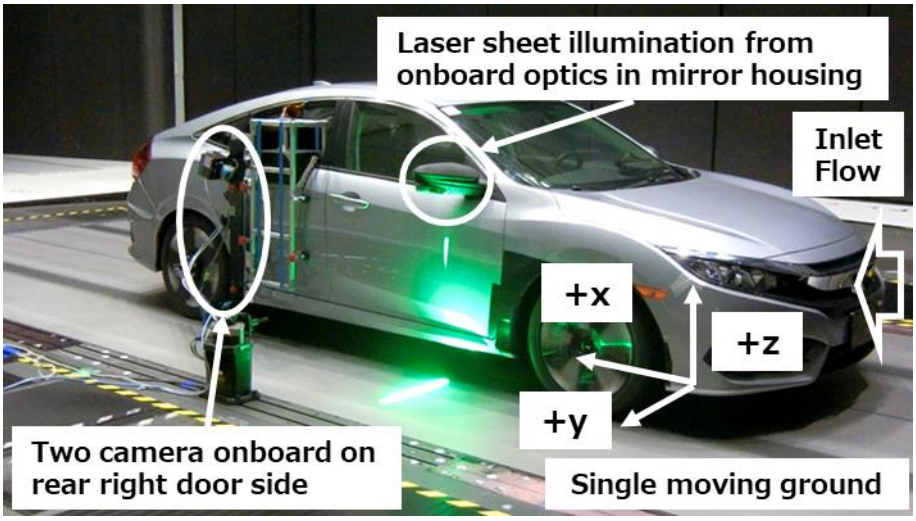

Fig. 1 Overview of wind tunnel testing under running with onboard PIV measurement system.

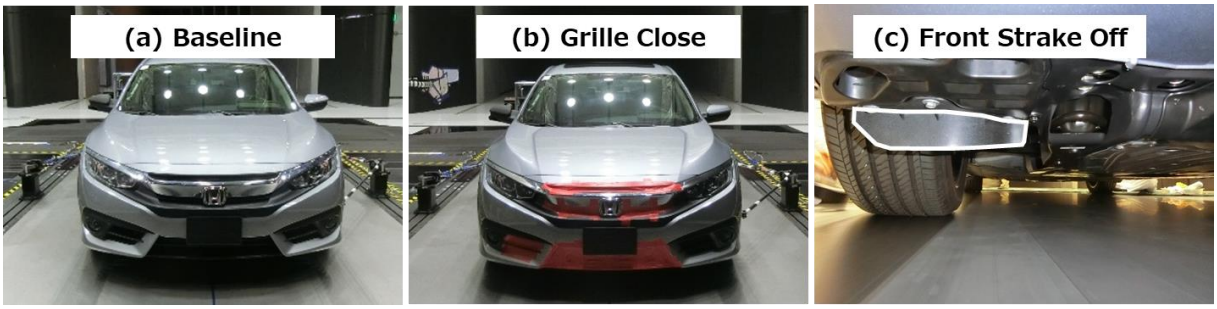

Fig. 2 Test vehicle configurations of (a) Baseline, (b) Grille Close and (c) Front Strake Off

Time averaged total pressure coefficients, Cp, distributions to comprehend the flow field are usually measured using total pressure tube rake with traverse system already installed on this facility. This measurement data can be validated with the following PIV measurement data. The measurement plane is as shown in Fig. 3 and consisted of 30 x 30 points in the y- and z-direction, over 10mm intervals. The pressure rake probe has 30 ports of sensors and the spacing of each sensor in *y*-direction is 10 [mm] with 1.575[mm] outer diameter and 1.321 [mm] inner diameter of

stainless tube. The data was averaged in 10 [seconds] for sufficient time averaged pressure profile. Two DSA3217 pressure scanners (F.S. 1 [psi], 16 [channels], Scanivalve Corporation) were used inside the traverse system.

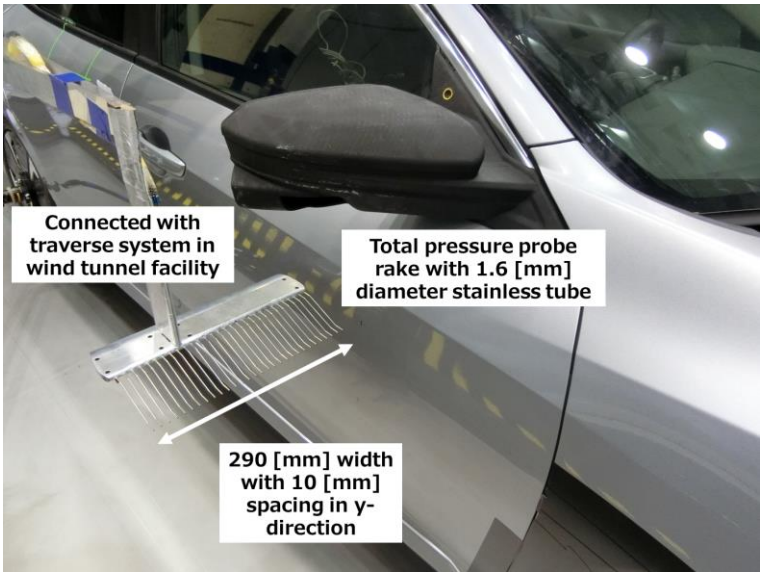

Fig. 3 Total pressure coefficient measurement by pressure tube rakes with traverse system.

2.3. Onboard High-speed 2D-3C PIV Measurement System

PIV measurement is known as a non-intrusive flow measurement and it is usually performed to measure the flow around the object by external optical access such as laser sheet, however, this laser sheet illumination causes the stronger laser light reflection on the surface of object. And the treating mat black aluminum on the surface of object, the pasting of the anti-reflective sheet on the surface of subject or reducing the laser power is selected to avoid the strong laser light reflection, respectively. This laser light reflection contributes to the deterioration of signal to noise ratio of the particle image. Therefore, in this study, onboard PIV measurement system as shown in Fig. 4 was proposed to avoid the stronger laser light reflection. These components of this onboard PIV are installed inside of the test vehicle as shown in Fig. 4. Laser source, laser, and camera synchronized controller (LC880, LabSmith) and control PC (DELL Precision T3610) are equipped inside of test vehicle and power supply and chiller of laser source are equipped in the trunk of test vehicle. This laser source is a high-repetition pulsed laser (18 [W], 1 [kHz], 527 [nm], DM20, Photonics Industries). These two high speed cameras (1024 x 1024 [pixels], miniAX200, Photoron) with Nikon f = 85 [mm] lens (AF-S NIKKOR 85mm f/1.4, Nikon Corporation) were installed on the right and rear side door of test vehicle to capture the y-z plane from downstream of measurement plane. Laser light sheet optics with optical fiber to transfer laser are installed in right

side mirror to illuminate the laser sheet around rotating front tire and wheel. As results, this optical configuration enables us to avoid the stronger laser light reflection on the exterior body surface as shown in Fig. 5. PIV Measurement area is 300 [mm] width and 300 [mm] around rotating front tire and wheel as shown in Fig. 4. This center point of measurement area is located at 150 [mm] horizontally from the surface of front door side panel and at 550 [mm] height from the ground due to keeping the pinch angle = 30 [deg.] between two cameras. The wind tunnel test conditions are shown in Table 1 with change in aerodynamic drag coefficient, C_D. Table 1 shows +3.8% increase in C_D in case of (c) Front Strake Off and -6.0% decrease in C_D in case of (b) Grille Close against (a) Baseline. The running speed was set to 100 [km/h] as free stream velocity. A large amount of uniform oil mist of about 3 [μm] can be generated by seeding generator including 4 nozzles (CTS-4000, SEIKA Digital Image Corporation). Dioctyl sebacate, DOS, is used for seeding oil and these oil mist can follow the flow and reduce the contamination of wind tunnel and test vehicles.

Table 1 Test vehicle configurations, conditions and change in C_D.

Case	Vinf [km/h]	Test vehicle configuration	$\Delta C_D/C_D$ [%]
(a)	100	Baseline	0
(b)		Grille Close	- 6.0
(c)		Front Strake Off	+ 3.8

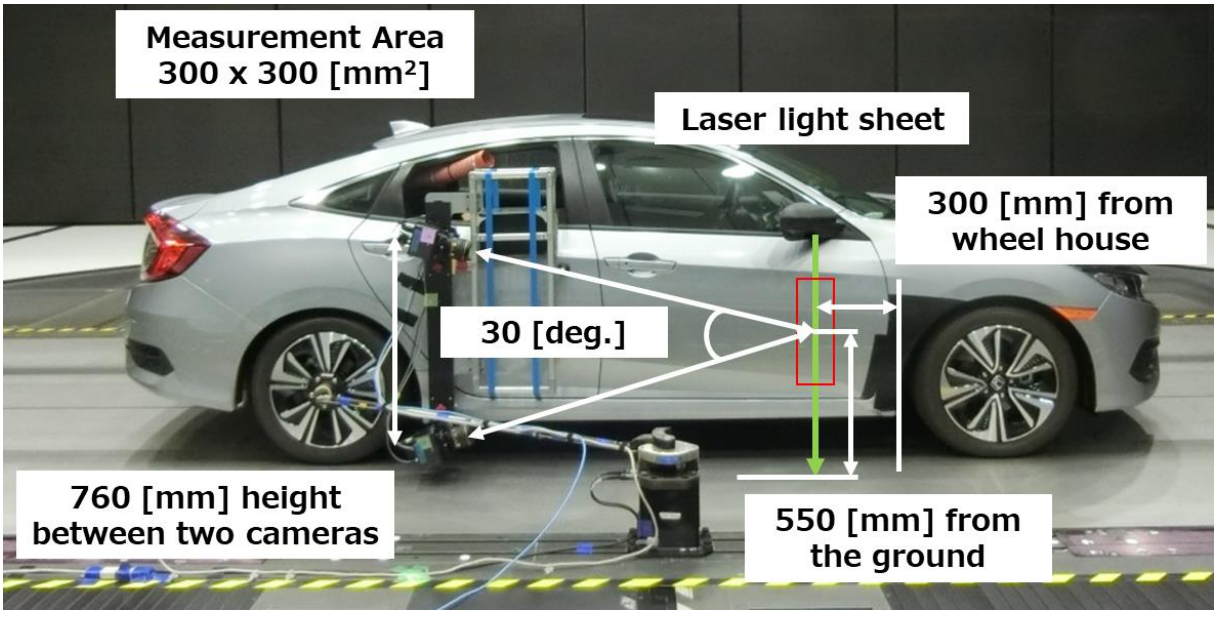

Fig. 4 Schematics of the onboard 2D-3C PIV measurement system.

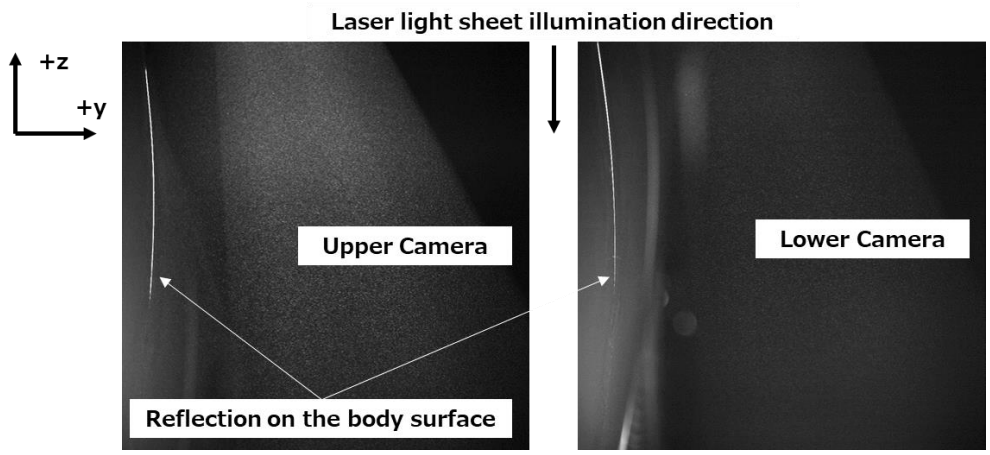

Fig. 5. Raw PIV image around body side by this onboard PIV to reduce the laser reflection.

Laser illumination pulse width is 40 [μsec] at frequency 800 [Hz]. Interrogation window size was 32 x 32 [pixels] with 50% overlap, the spacing between vectors was in y-direction and z-direction was 5.40 [mm] as a result. Each 2700 shots of time series particle images were measured at 800 [Hz] during about 3.5 [seconds]. These image data were stored in about 15 [minutes] and only 100 paring data were analyzed for quick review in 10 [minutes]. Koncerto II (SEIKA Digital Image Corporation) was used for measurement control and analyzing the velocity field. After that, the data analysis as post processing is operated by MATLAB and Python to execute POD analysis.

3. Results and Discussions

3.1. Wake Patterns around Front Tire and Wheel

Total pressure measurement is easily performed at development phase to investigate the overall flow field, for example, rear wake behind test vehicle and side wake around it, as shown in Fig. 6. They help us easily inspect the different wake patterns. In particular, the front wheelhouse wake in case of (b) Grille Close was smaller than that of (a) Baseline. This wake pattern was caused by decrease in mass flow rate from the engine room due to the decrease in the incoming cooling flow and the increase in the mass flow rate in underfloor.

On the other hand, the front wheelhouse wake in case of (c) Front Strake Off was larger than that of (a) Baseline, because there was a higher-pressure field in wheelhouse by diminishing the lower-pressure field behind Front Strake. Especially, there were smaller tire wake near ground in case of (c) Front Strake Off than that of (a) Baseline and (b) Grille Close, because it depends on the pressure field in the wheelhouse. This wake phenomenon around front tire and wheel behaves like a whack-a-mole.

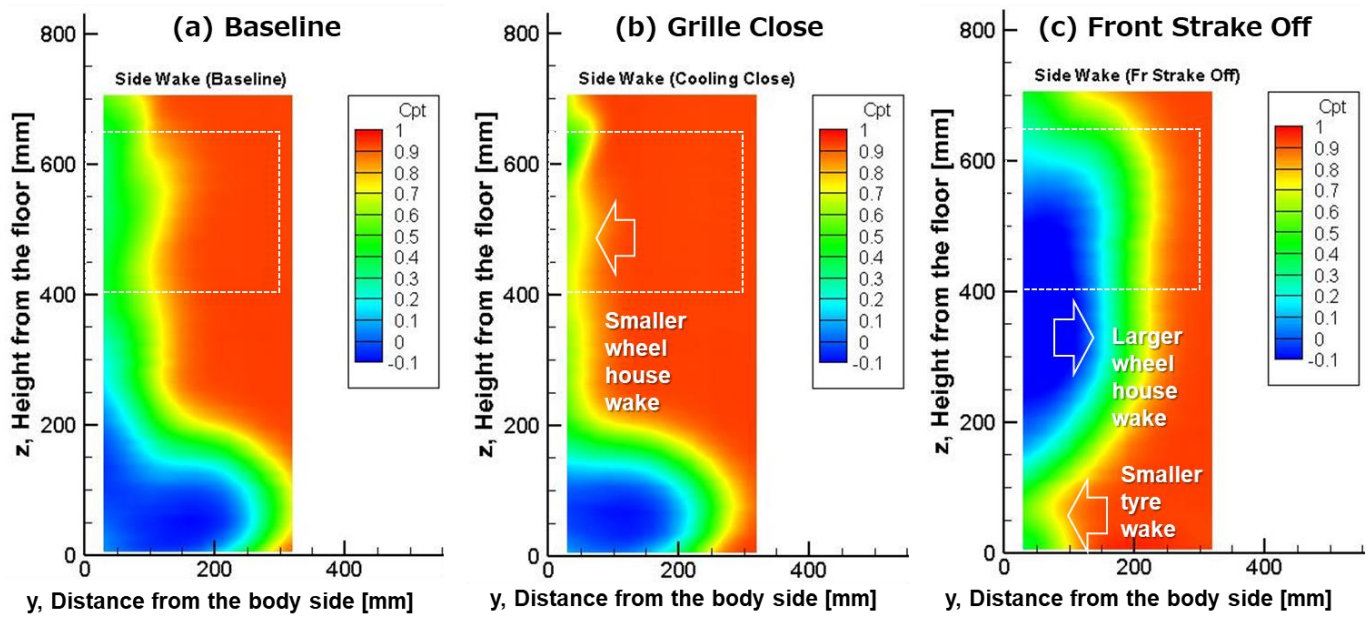

Fig. 6 Total pressure coefficient (Cpt) field around front wheelhouse of (a) Baseline, (b) Grille Close and (c) Front Strake Off and white dot line shows onboard PIV measurement area in Fig. 7

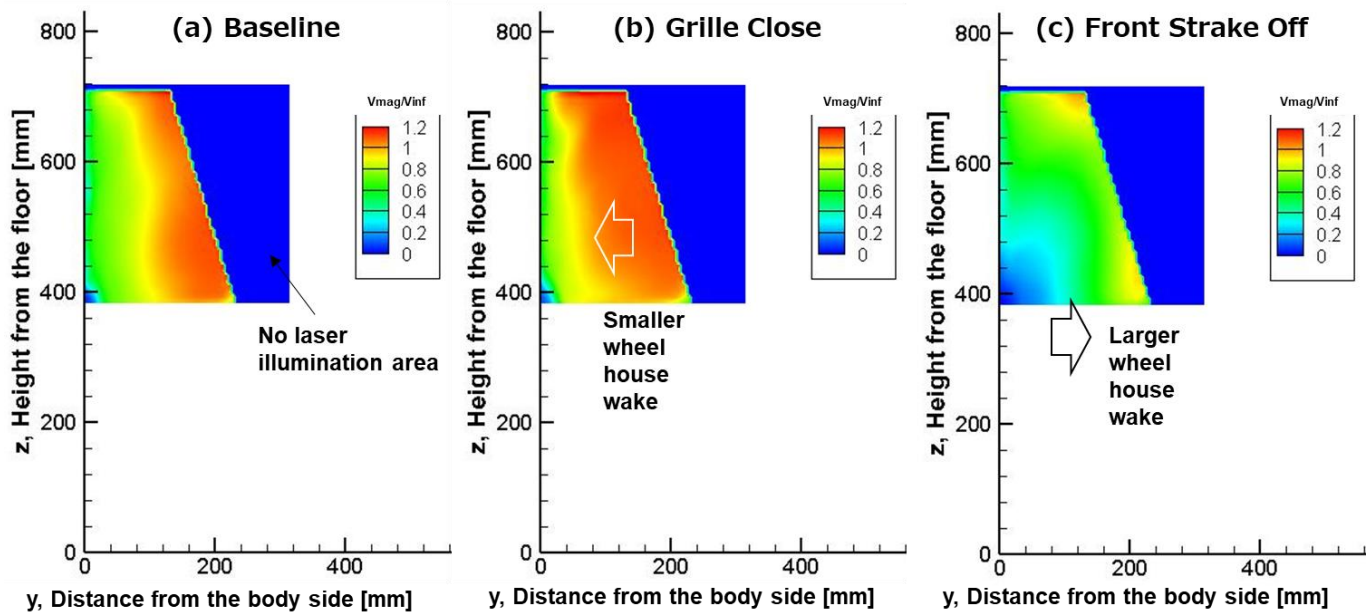

Fig. 7 Time averaged velocity magnitude field around front wheelhouse of (a) Baseline, (b) Grille Close and (c) Front Strake Off

3.2. Onboard PIV Measurement Validation

This onboard PIV measurement proposed in this study is validated by comparison with total pressure coefficient profile by total pressure probe rake measurement, as shown in Fig. 3. The time averaged velocity magnitude fields by this onboard PIV measurement are shown in Fig. 7. Here,

the normalized velocity magnitude by free stream velocity is used to compare with Cp distribution shown in Fig. 6. They show that there are very similar wake patterns around front wheelhouse under all these aerodynamic configurations. In particular, this onboard PIV measurement can also detect the smallest wheelhouse wake in case of (b) Grille Close and the largest one in case of (c) Front Strake Off, same as Fig. 6. It shows that this onboard PIV measurement can exhibit sufficient measurement accuracy.

3.3. Front Wheelhouse Wake Characteristics

The time averaged velocity magnitude field enable us to understand the wake size and wake generation from the point of view of the kinetic energy of the overall flow, as shown in Fig. 7. Moreover, these standard deviations of velocity magnitude field are shown in Fig. 8. with the time averaged velocity magnitude field to investigate the change in turbulent intensity by flow interaction between front wheelhouse wake and main flow. There is main flow with lower turbulent intensity as shown in (a) Baseline. Smaller front wheelhouse wake, remarkable lower turbulent intensity under (b) Grille Close. There is larger front wheelhouse wake with remarkable higher turbulent intensity under (c) Front Strake Off.

So far, the size, generation and turbulent intensity of front wheelhouse wake were discussed by time averaged and standard deviation of velocity magnitude, qualitatively. Additionally, to evaluate these front wheelhouse wake characteristics quantitatively, these two measurement points are selected from PIV measurement plane; P1 is in main flow area and P3 near body side flow area, as shown in Fig. 9. And normal distributions of each velocity component; u streamwise, v lateral and w vertical velocity components, are shown in Fig. 10.

The widths of this normal distributions of each velocity component in case of (b) Grille Close are smallest of all cases at both P1 and P3. There is main flow not affected by front wheelhouse wake. On the other hand, there are apparently widest widths of this normal distributions of each velocity component in case of (c) Front Strake Off. Especially, in case of (c) Front Strake Off, there is remarkably decrease in streamwise velocity and broadest lateral and vertical velocity distributions at P3 that shows higher turbulent intensity and largest wake produced from front wheelhouse due to the lack of negative pressure in wheelhouse by Front Strake Off.

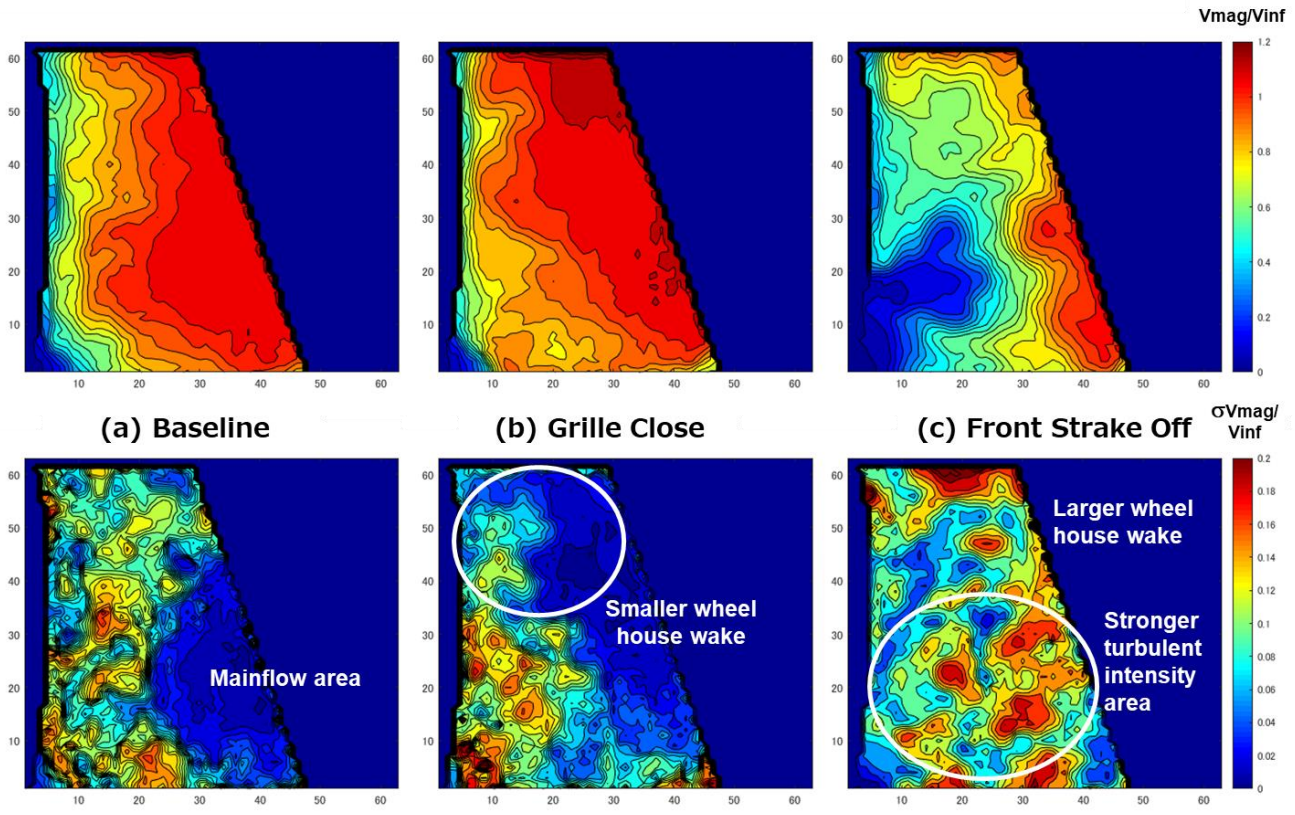

Fig. 8 Time averaged and standard deviations of velocity magnitude flow field under (a) Baseline, (b) Grille Close and (c) Front Strake Off

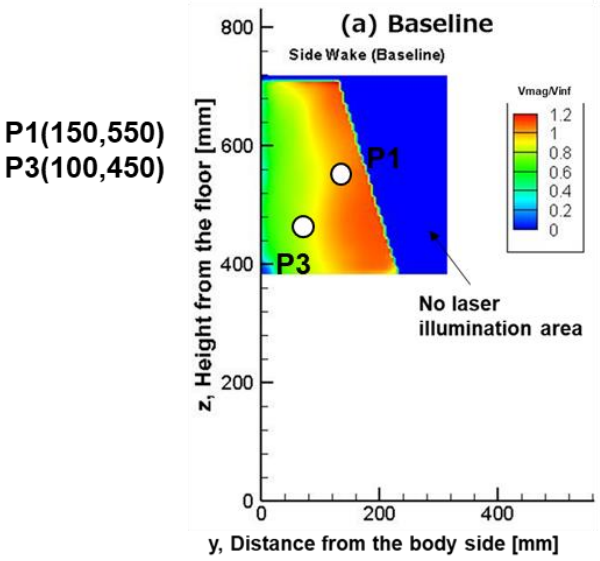

Fig. 9 Selected measurement points, Point 1 & 3 location in PIV measurement yz-plane

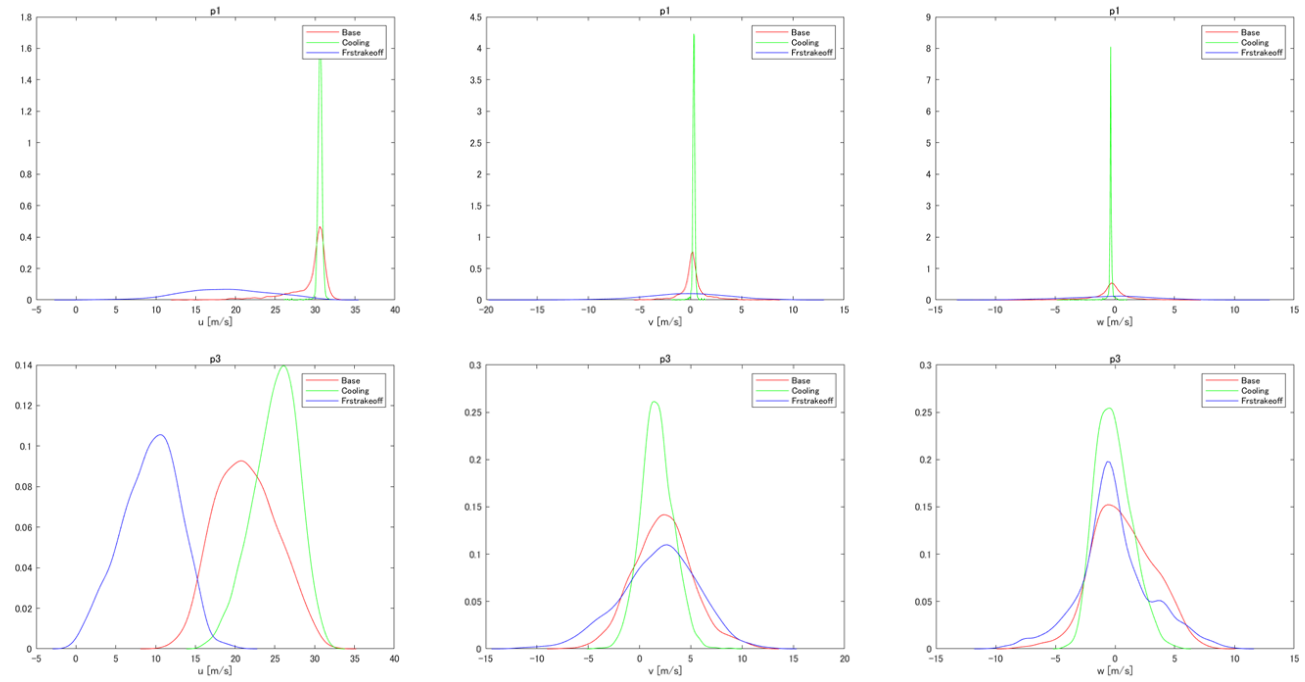

Fig. 10 Normal distribution of each velocity component; u streamwise, v lateral and w vertical velocity components, at Point 1 in main flow area and Point 3 near body side flow area under (a) Baseline, (b) Grille Close and (c) Front Strake Off

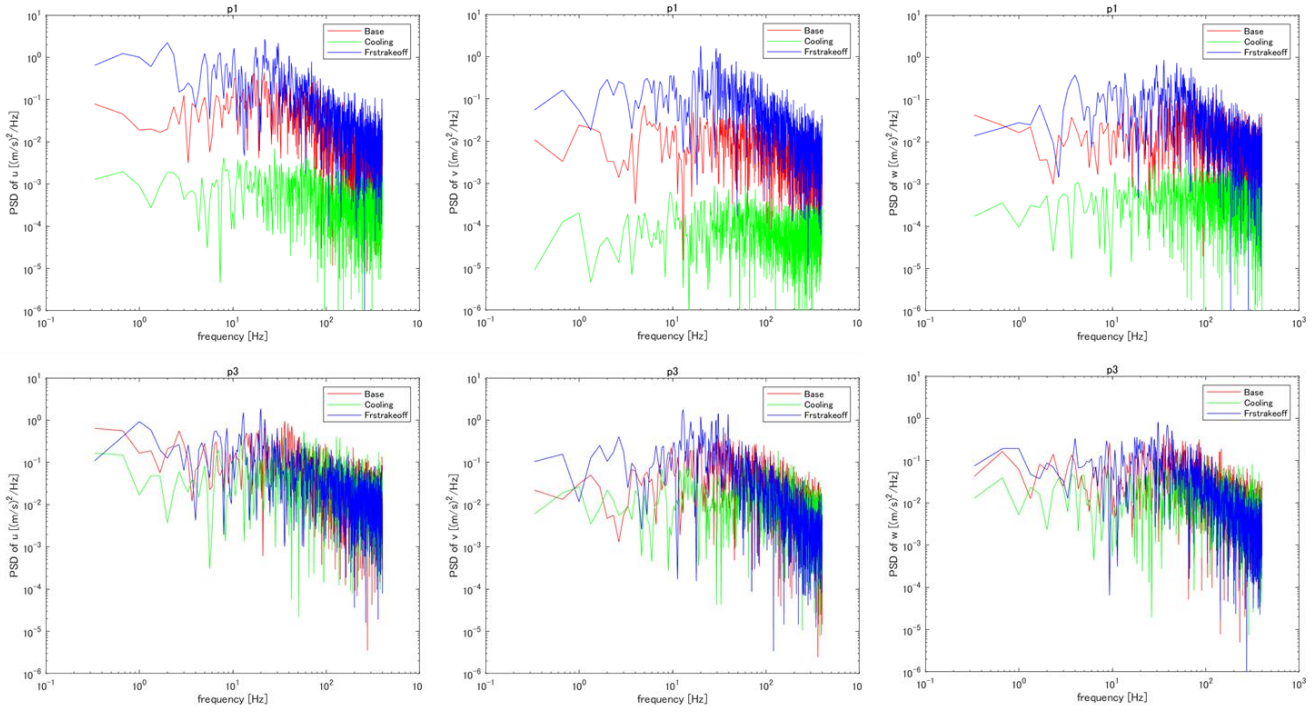

Fig. 11 Power spectrum density of each velocity component; u streamwise, v lateral and w vertical velocity components, at Point 1 in main flow area and Point 3 near body side flow area under (a) Baseline, (b) Grille Close and (c) Front Strake Off

3.4. Front Wheelhouse Wake Fluctuation

In this section, frequency analysis of this onboard PIV measurement data at the mentioned selected points was performed to investigate the predominant frequency and power spectrum density of each velocity component in front wheelhouse wake. Power spectrum density, PSD of each velocity component at P1 and P3 are shown in Fig. 11 to compare with aerodynamic configurations. Fig. 11 shows that there is remarkably highest level of PSD over all frequency range in case of (c) Front Strake Off. It clarifies that front wheelhouse wake fluctuation of each velocity component is enhanced by (c) Front Strake Off in front of front tire. On the other hand, there is lowest fluctuation level in case of (b) Grille Close not only at P1 in main flow but also at P3 in near body side.

3.5. POD Analysis of Front Wheelhouse Wake by Onboard PIV Measurement

Currently, proper orthogonal decomposition: POD analysis is used to extract the mode of flow field and understand the features, especially from tremendous CFD data (Taira 2017). In this study, this POD analysis of velocity magnitude by this onboard PIV measurement was applied to investigate the featuring modes of these complicated flow around front wheelhouse, as shown in Fig. 12. These figures show 15 POD modes of velocity magnitude under all aerodynamic configurations. At first, POD mode #1 and #2 show two large vortices but located differently in this wake under all cases and correspond to the higher turbulent kinetic energy in this wake. On the other hand, higher POD modes show some smaller vortices with lower one. Moreover, in case of (b) Grille Close, there is more clear and smaller vortices patterns compared to the other two cases, as shown in POD modes from #5 to #10. These POD modes indicate the lower kinetic energy in this wake. These clear POD modes emphasize the different aerodynamic performance between (a) Baseline and (b) Grille Close configurations.

The eigenvalues derived from POD analysis are accumulated to estimate the flow kinetic energy (Taira 2017). The relationship between this flow kinetic energy and POD modes is plotted as shown in Fig. 13. This figure clearly shows the lowest kinetic energy in all mode range in case of (b) Grille Close that shows the lowest drag compared with the other cases. For example, in the same POD mode#8, there is the smallest flow kinetic energy with smaller vortices in case of (b) Grille Close to compare the other configurations with larger vortices. There is complicated flow around front wheelhouse due to the three-dimensional flow are created by front wheelhouse wake fed from the gap between the rotating tire and wheel arch, the wheel wake fed from rotating wheel spork and accelerated main flow along the front bumper. Each POD modes have a small kinetic flow energy with small vortices unlike the simple flow such as NACA0012 airfoil (Taira 2017).

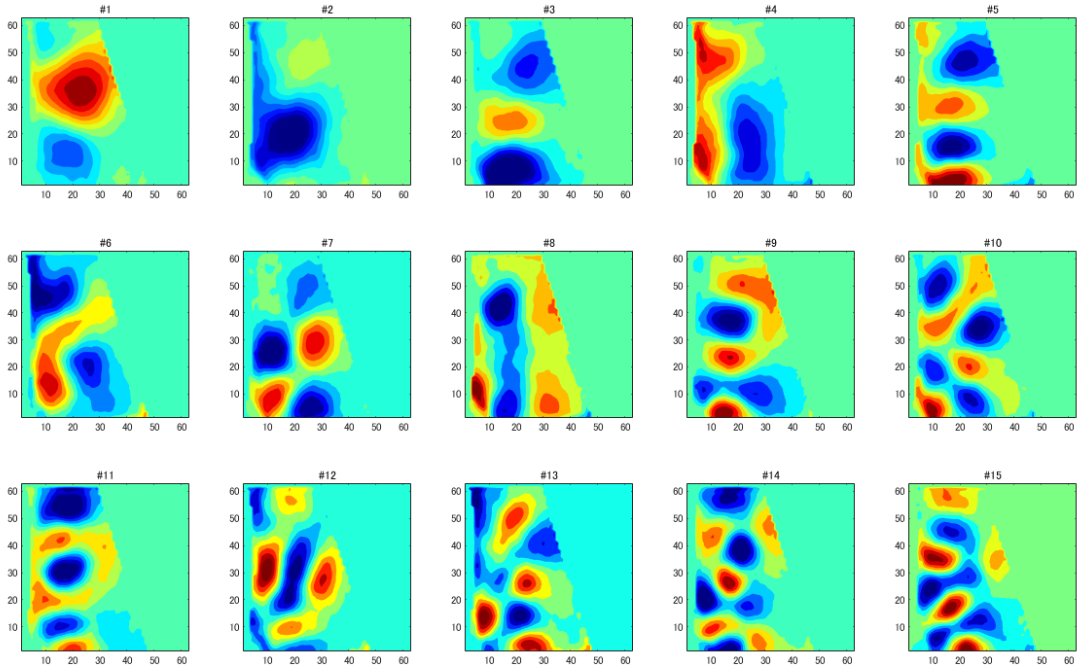

Fig. 12 (a) POD modes from #1 to #15 of velocity magnitude by onboard PIV measurement around front wheelhouse in case of (a) Baseline

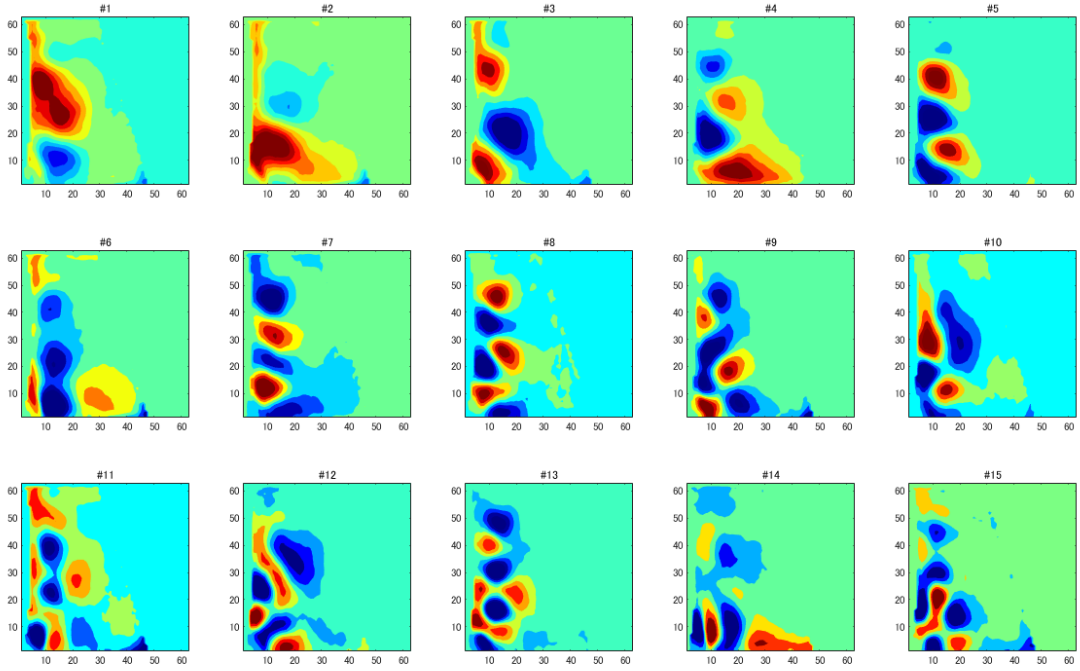

Fig. 12 (b) POD modes from #1 to #15 of velocity magnitude by onboard PIV measurement around front wheelhouse in case of (b) Grille Close

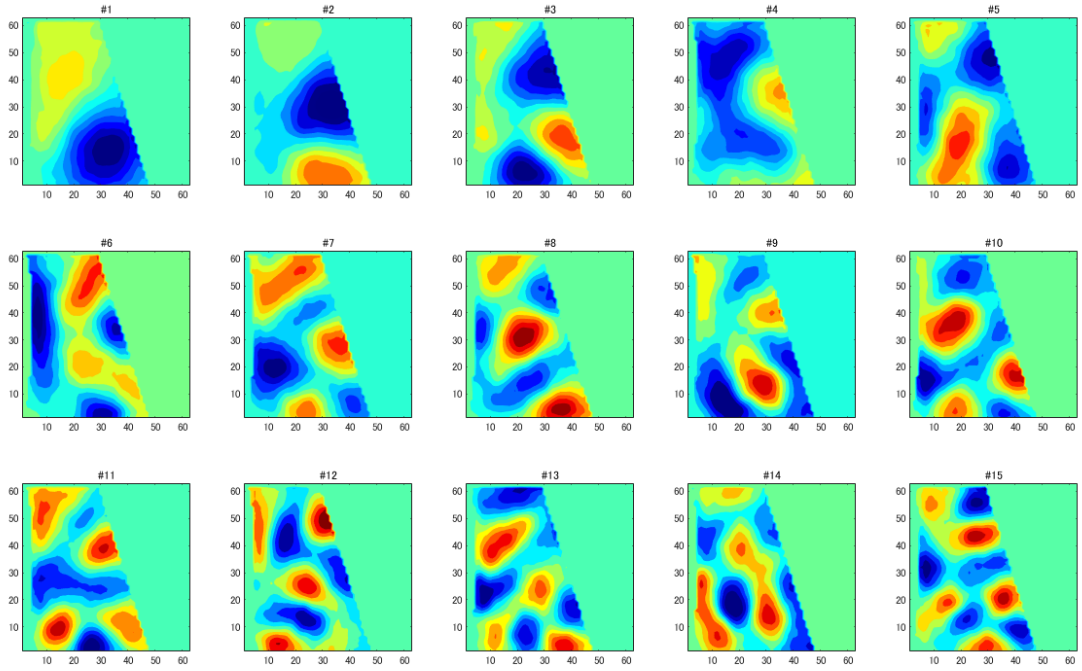

Fig. 12 (c) POD modes from #1 to #15 of velocity magnitude by onboard PIV measurement around front wheelhouse in case of (c) Front Strake Off

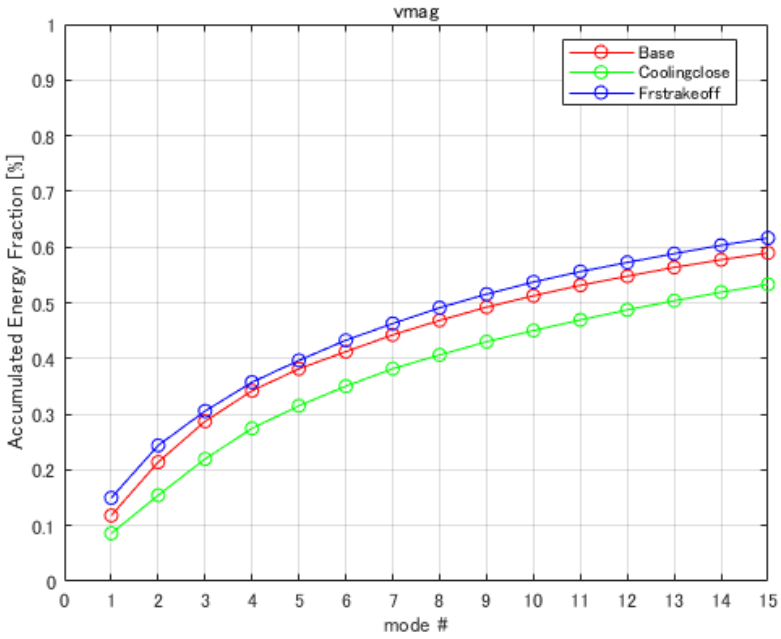

Fig. 13 Flow kinetic energy accumulated by eigenvalues of POD modes

4. Conclusions

This cutting-edge onboard 2D-3C PIV measurement system has been developed in wind tunnel facility in this study. There are more clear time-series particle images captured by this system than that of usual optical access from outside of the object. This onboard PIV measurement enable us to investigate the temporal and spatial wake patterns and behaviors around front wheelhouse on vehicle aerodynamic performance.

The time averaged velocity magnitude fields shows that this onboard PIV measurement demonstrated sufficient measurement accuracy with Cp distribution as compared to total pressure probe rakes, for example, the smaller wheelhouse wake under Grille Close and the larger wheelhouse wake under Front Strake Off. And so, this measured standard deviation of velocity magnitude shows the flow fluctuation due to the front wheelhouse wake and flow interaction between main flow and front wheelhouse wake.

The featuring modes in the complicated flow around front wheel have been extracted by POD analysis of this onboard PIV measurement data. This front wheelhouse wake has strong effect on change in the aerodynamic drag. The eigenvalues derived from POD analysis are accumulated to estimate the flow kinetic energy. Each POD modes have a small kinetic flow energy with small vortices due to the three-dimensional flow around front wheelhouse. As result, the front wheelhouse wake with smaller vortices in lower POD modes have lower drag performance.

5. Future works

This study on application of on-board PIV measurement to investigate the side wake on vehicle aerodynamics shows that this measurement technique has a great potential to apply to real world condition under running while providing homogenous seeding particles around vehicle, minimizing flow interaction with camera, providing high voltage to the laser source from the large capacity battery in vehicle and protecting the test driver from the laser. And these POD analysis on the other velocity components have not been sufficiently performed; however, this study shows the great potential to clarify the flow phenomena deeply on vehicle aerodynamics by POD analysis of onboard PIV measurement. In particular, more feature in this complicated flow can be extracted by POD, DMD and the other data science techniques such as network-based analysis (Taira 2022)

and as result, improvement in vehicle aerodynamic performance and vehicle dynamics will be achieved by capturing the features of the flow.

6. Acknowledgements

The wind tunnel test operation and preparation for test model drawing were supported by Mr. Shota Takigawa, Mr. Katsuki Maeda and Mr. Satoshi Nakamura, as guest engineers. The POD analysis and this manuscript review were supported by Mr. Nucera Fortunato. Their careful works are greatly acknowledged by all authors.

7. References

- Ambo, K., Yoshino, T., Kawamura, T., Teramura, M., Philips, D. A., Brès, G. A., & Bose, S. T. (2017). Comparison between Wall-modeled and Wall-resolved Large Eddy Simulations for the prediction of boundary-layer separation around the side mirror of a full-scale vehicle. In *55th AIAA Aerospace Sciences Meeting* (p. 1661).
- Ambo, K., Nagaoka, H., Philips, D. A., Ivey, C., Brès, G. A., & Bose, S. T. (2020). Aerodynamic force prediction of the laminar to turbulent flow transition around the front bumper of the vehicle using Dynamic-slip wall model LES. In *AIAA Scitech 2020 Forum* (p. 0036).
- Elofsson, P., & Bannister, M. (2002). Drag reduction mechanisms due to moving ground and wheel rotation in passenger cars. *SAE Transactions*, 591-604.
- Haff, J., Lange, S., & Wilhelmi, H. (2017). An Experimental Study of the Under-Floor Flow of a VW Golf 7 under On-Road and Wind-Tunnel Conditions via Particle Image Velocimetry. *11th FKFS conference: Progress in Vehicle Aerodynamics and Thermal Management*
- Hurlbrink, J., Barth, T., Lietmeyer, C., Wittmaier, A., & Seume, J. (2019). Analysis of the Flow Topology and Loss Mechanisms in the Wheel-house Area. *12th FKFS conference: Progress in Vehicle Aerodynamics and Thermal Management*
- Koremoto, K., Kawamura, N., Kuratani, N., Nakamura, S., Arai, T., Galanga, F., & Muller, S. (2010, October). The Characteristics of the Honda Full Scale Aero-acoustic Wind Tunnel equipped with a Rolling Road System. In *8th MIRA International Vehicle Aerodynamics Conference*

- Koremoto, K., Kawamura, N., Aoki, M., Kuratani, N., Nakamura, S., & Yoshioka, H. Full-scale Wind Tunnel Equipped with Single-belt Rolling Road System. *Honda R&D Technical Review*, 23(1), 18-22.
- Taira, K., Brunton, S. L., Dawson, S. T., Rowley, C. W., Colonius, T., McKeon, B. J., & Ukeiley, L. S. (2017). Modal analysis of fluid flows: An overview. *AIAA Journal*, 55(12), 4013-4041.
- Taira, K., & Nair, A. G. (2022). Network-based analysis of fluid flows: Progress and outlook. *Progress in Aerospace Sciences*, 131, 100823.
- Takeuchi, K., Kawamura, T., Kuratani, N., Kobayakawa, A., Osawa, Y., & Tsubokura, M. (2016). LES on the aerodynamic effect of tire shapes with moving ground using a detailed full-scale vehicle model. *International Conference on Vehicle Aerodynamics 2016*
- Wäschle, A. (2007). The influence of rotating wheels on vehicle aerodynamics-numerical and experimental investigations (No. 2007-01-0107). *SAE Technical Paper*.